UC Davis REU Final Report

Tao You

January 28, 2023

Abstract

We calculate the susceptibility, equal-time structure factor and entanglement entropy for quantum spin glasses of sizes 8, 9, 10, 12 and 16 sites as a function of the transverse magnetic field strength, and compare it to the Linked Cluster series expansion method obtained by Young and Singh [1]. We also calculate the local susceptibility χ_{ii} for different transverse field values, and computationally confirm that at high fields the distribution of local susceptibility approaches Gaussian. Going from high field to low field, we identify the long-tailed distribution in the Griffiths phase and the large local susceptibilities in the spin glass phase. Lastly, as an on-going project, we also employ perturbation theory to mainly target studying entanglement entropy at very low field values, but this method has its obvious limitations regarding the size of the system and the field strength that we can study. Here, we simply present some results that we have calculated using perturbation theory.

Date Accepted: _____

Contents

I Spin glass review

In this project we consider the Transverse Field Ising (TFI) spin glass, where the classical spin-spin coupling energies follow the random bimodal distribution. It Hamiltonian is the sum of the classical part and the quantum part:

$$H = H_0 + H_1. \tag{1}$$

The classical Ising Hamiltonian is

$$H_0 = -\sum_{\langle i,j \rangle} J_{ij}\sigma_i^z\sigma_j^z \tag{2}$$

where $J_{ij} \in \{+1, -1\}$ (bimodal distribution) and the quantum Hamiltonian is

$$H_1 = -h_x \sum_i \sigma_i^x. \tag{3}$$

We aim to measure the spin glass susceptibility under the TFI model for 2D nearest-neighbor finite clusters (e.g. 3 by 3, 4 by 4) using exact diagonalization. Roughly speaking, for any given transverse field value h_x, the spin glass susceptibility is computed by diagonalizing the Hamiltonian with an added longitudinal field h_z^k (see the following section for details).

II Local susceptibility χ_{ii}

In general, susceptibility is a measurement of how "susceptible" (how rapidly does it change) the magnetization of the system is in response to external magnetic fields. Thus, in order to calculate the magnetic susceptibility of an individual site on a lattice, we need to further perturb the system with a longitudinal field on a single site, yielding the new Hamiltonian

$$H[\{h_z^k\}] = -\sum_{\langle i,j \rangle} J_{ij}\sigma_i^z\sigma_j^z - h_x \sum_i \sigma_i^x + \sum_k h_z^k \sigma_k^z \tag{4}$$

where $\{h_z^k\}$ denotes the vectorized longitudinal field strength with k as the looping index. Fixing k and setting the longitudinal fields on all other sites to zero (thus $\{h_z^k\} = \{0, \ldots, 0, h_z^k, 0, \ldots, 0\}$), the second-order perturbation theory gives the definition and the analytical method of calculating the local susceptibility for the kth spin. Now the unperturbed Hamiltonian is

$$H_0' = H_0 + H_1 = -\sum_{\langle i,j \rangle} J_{ij}\sigma_i^z\sigma_j^z - h_x \sum_i \sigma_i^x. \tag{5}$$

and the perturbing Hamiltonian is

$$H_1' = \sigma_k^z \tag{6}$$

scaled by the longitudinal field strength h_z^k. The second order perturbative expansion of the ground energy $E_0[h_z^k]$ gives

$$E_0[h_z^k] = E_0[0] + h_z^k \langle 0|\sigma_k^z|0\rangle + (h_z^k)^2 \sum_n \frac{|\langle 0|\sigma_k^z|n\rangle|^2}{E_0 - E_n}. \tag{7}$$

The local susceptibility χ_{kk} is defined as the second-order coefficient in the perturbative expansion

$$\chi_{kk} = -\sum_n \frac{|\langle 0|\sigma_k^z|n\rangle|}{|E_0 - E_n|}. \tag{8}$$

Note that the first order term must always vanish due to spin inversion symmetry.

In numerical study, the Implicitly Restarted Lanczos Method (IRLM) is used to diagonalize Hamiltonian matrices. It is very good at obtaining the extremal values of the spectrum very quickly. Thus, we can equate the perturbative expansion with a Taylor series for a numerically feasible way of calculating the susceptibility. The Taylor expansion of its corresponding lowest eigenenergy $E_0[\{h_z^k\}]$ to second order gives

$$E_0[\{h_z^k\}] = E_0[\{0\}] + \sum_k h_z^k \cdot \left(\frac{dE_0[\{h_z^k\}]}{dh_z^k}\right)_{h_z^k=0} + \sum_k \frac{h_z^{k2}}{2} \cdot \left(\frac{d^2E_0[\{h_z^k\}]}{dh_z^{k2}}\right)_{h_z^k=0}. \tag{9}$$

Fixing k and setting all other longitudinal fields to zero, we obtain the single site susceptibility and order parameter

$$\begin{aligned} E_0[\{h_z^k\}] &= E_0[\{0\}] + h_z^k \cdot \left(\frac{dE_0[\{h_z^k\}]}{dh_z^k}\right)_{h_z^k=0} + \frac{h_z^{k2}}{2} \cdot \left(\frac{d^2E_0[\{h_z^k\}]}{dh_z^{k2}}\right)_{h_z^k=0} \\ &= E_0[\{0\}] + \frac{h_z^{k2}}{2} \cdot \left(\frac{d^2E_0[\{h_z^k\}]}{dh_z^{k2}}\right)_{h_z^k=0}. \end{aligned} \tag{10}$$

As we have shown above, the first order term is again zero, which gives the formula for calculating the local susceptibility

$$\chi_k = \frac{2(E_0[h_z^k = 0] - E_0[h_z^k])}{(h_z^k)^2}. \tag{11}$$

We calculate the distribution of local susceptibility for all spin and different sizes as a function of the transverse field value h_x. The result shows a normal distribution at high fields just as expected

(see Fig. (1)), since the local susceptibility of any individual site i is largely determined by the bond energy J within its neighborhood, and it is the disorder of the bond energy that gives rise to the normal distribution of local susceptibility. Notice that the peak of the distribution lies rough at $1/(h_x/J)$.

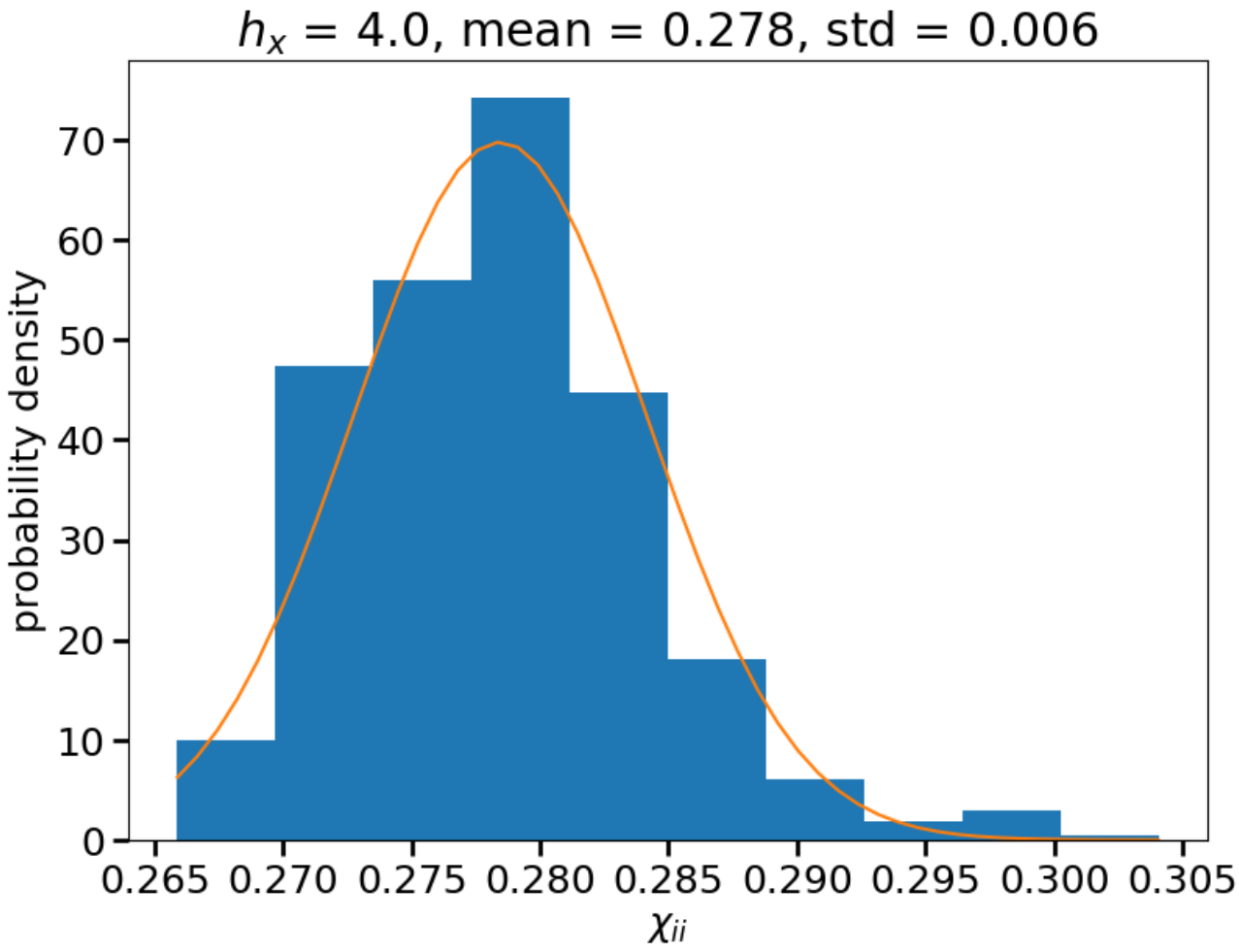

Fig. 1. The local susceptibility distribution across sizes 8, 9, 10, 12, and 16 for 100 instances each at $h_x/J = 4.0$.

Between $h_x = 0.8$ and $h_x = 4$, the spin glass lies in the Griffiths-McCoy (MC) phase where we begin to see the long tail developing on top of the normal distribution (see Fig. (2)); this is the key signature of MC phase as the rare regions—regions within the spin glass where the spins are locally ferromagnetic and the quantum fluctuations vary slowly between up and down state—will produce some small finite fraction of spins with very large local susceptibilities.

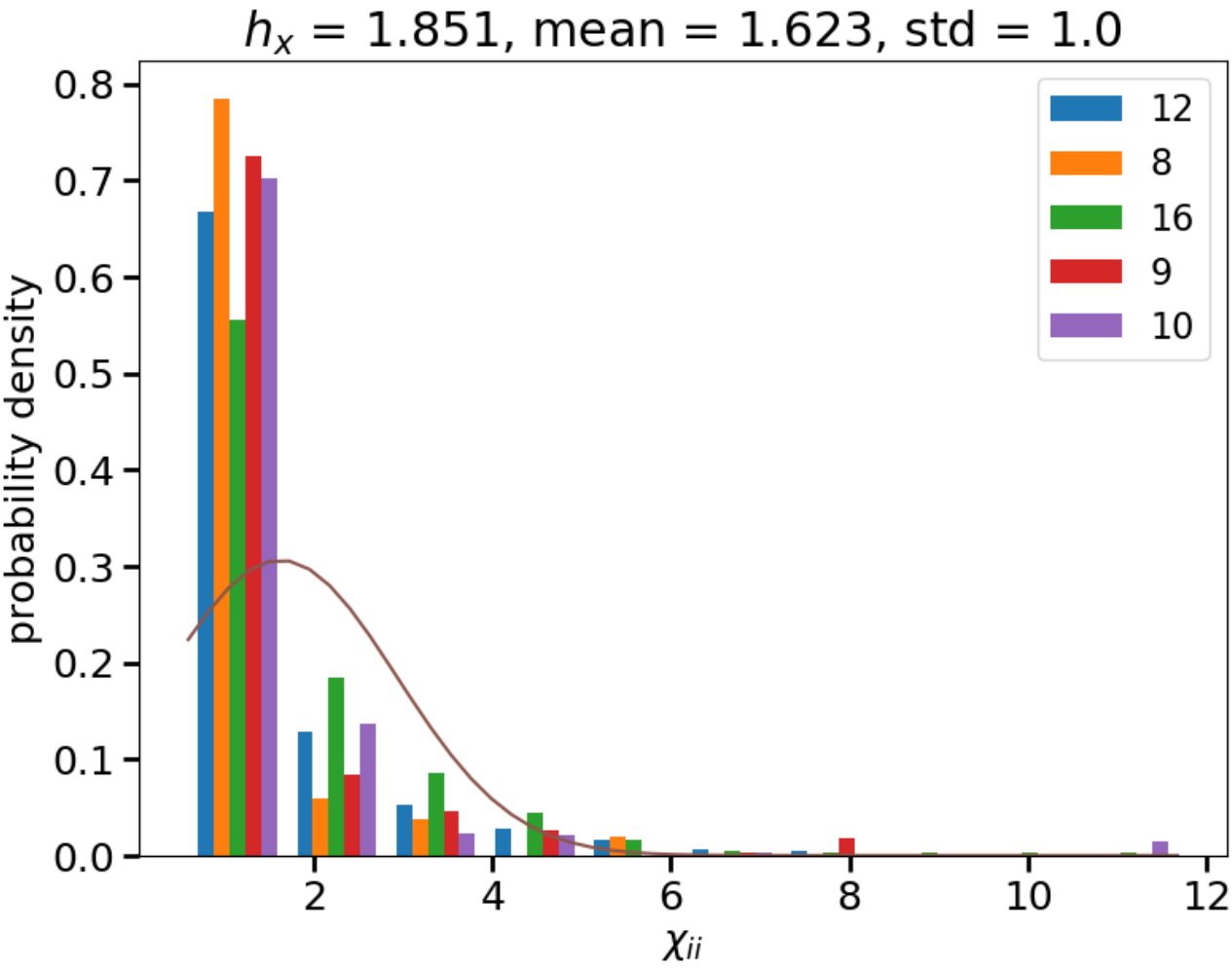

Fig. 2. The local susceptibility distribution across sizes 8, 9, 10, 12, and 16 for 100 instances each at $h_x/J = 1.851$.

As we lower the transverse field and the system is deep Within the spin glass phase $h_x < 0.8$, the number of spins with large local susceptibility becomes larger and grows up to be a finite fraction of the total size of the system (see Fig. (3)).

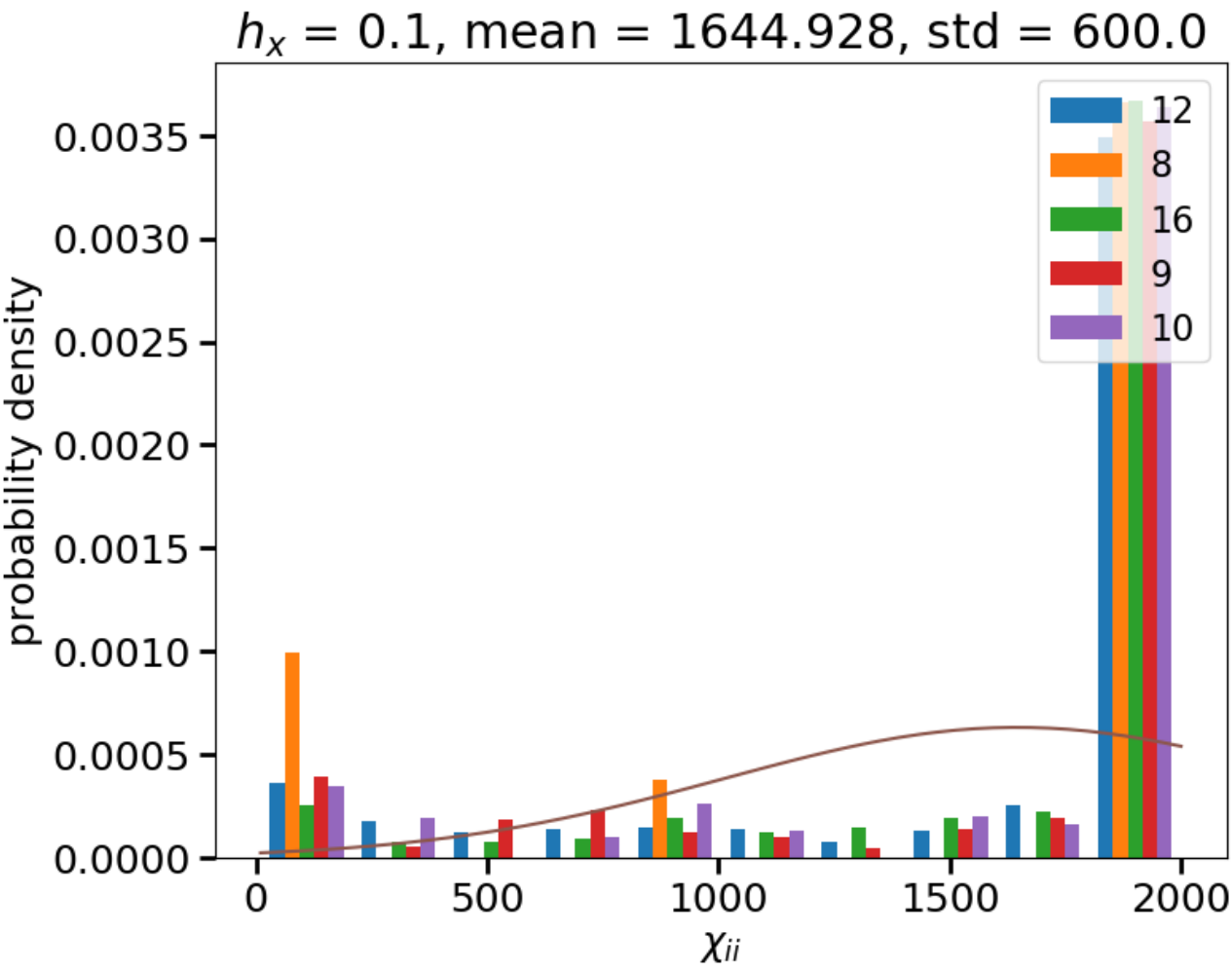

Fig. 3. The local susceptibility distribution across sizes 8, 9, 10, 12, and 16 for 100 instances each at $h_x/J = 0.1$.

Exactly how this occurs is complex, but a similar phenomenon is seen in the Ising model without disorder at low fields where the ground state is given by the Schrodinger's cat state:

$$|+\rangle = \frac{1}{\sqrt{2}}(|\uparrow\rangle + |\downarrow\rangle)$$
$$|-\rangle = \frac{1}{\sqrt{2}}(|\uparrow\rangle - |\downarrow\rangle)$$

where $|\uparrow\rangle$ and $|\downarrow\rangle$ denote "all up" and "all down" state respectively with their energy difference as h_x^N. At the thermodynamic and low-field limit, this energy difference becomes so small that the two states are nearly-degenerate. To see this, consider the matrix elements $\langle\psi'|\sigma_i^z|\psi\rangle = 1$ for $\psi \neq \psi'$ and 0 for $\psi = \psi'$ where $\psi, \psi' \in \{+, -\}$. Equating the Eq. (4) with the second order perturbative expansion

of the energy $E[h_z]$ tells us that

$$E_0[h_z = 0] - \frac{1}{2}\chi_{ii}(h_z^k)^2 = \langle 0|H_0|0\rangle + (h_z^k)^2 \sum_n \frac{\langle 0|\sigma_i^z|n\rangle^2}{E_g - E_n}$$
$$-\frac{1}{2}\chi_{ii}(h_z^k)^2 = (h_z^k)^2 \sum_n \frac{|\langle 0|\sigma_i^z|n\rangle|^2}{E_g - E_n}$$
$$\chi_{ii} = 2\sum_n \frac{|\langle 0|\sigma_i^z|n\rangle|^2}{E_n - E_g}. \tag{12}$$

For a system of size N and transverse field h_x, the ground energy is $-h_x^N$ and the first excited energy is h_x^N, yielding an energy difference of $2h_x^N$. Now it is not difficult to see that the susceptibility blows up at low fields because the energy gap is vanishingly small.

We are interested in the statistical quantities of the local susceptibility distribution change as we vary the transverse field. Here, we present the numerical calculations for the mean, standard deviation (Figure 4) as well as the lognormal variance (Figure **??**) and compare them to the series expansion result obtained by Singh and Young.

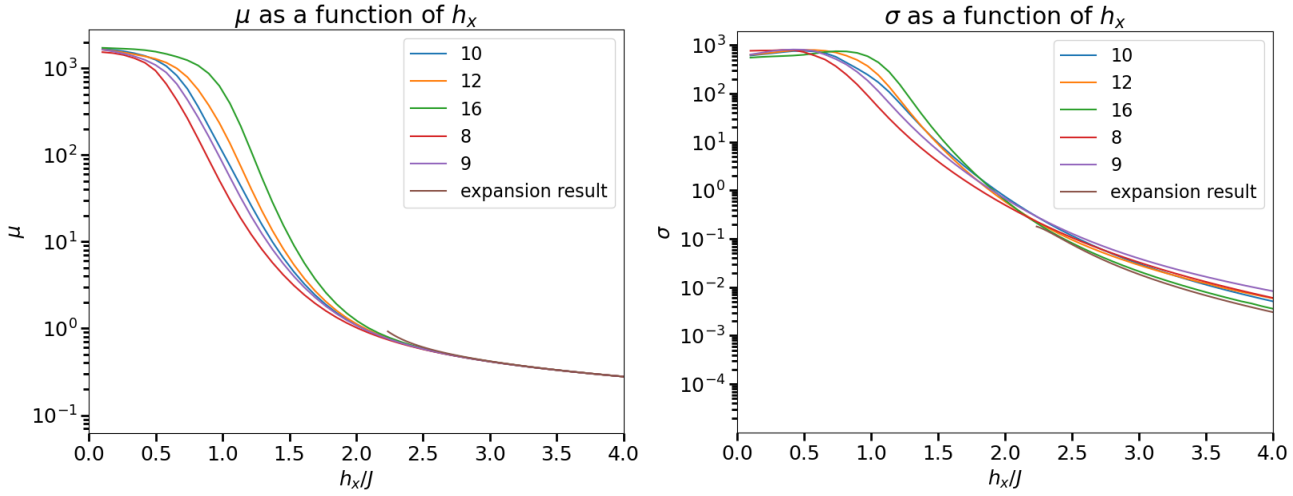

Fig. 4. Mean (left) and standard deviation (right) of local susceptibility as a function of h_x for systems of $8, 9, 10, 12, 16$ spins.

We also compute the lognormal variance assuming that the distribution is lognormal whereas in reality this may well not be the case. Nevertheless, for each h_x value, the lognormal variance σ^2 is computed using the formula

$$\sigma^2(h_x) = \log\left(\frac{\text{Var}[X(h_x)]}{\text{E}[X(h_x)^2]} + 1\right) \tag{13}$$

where $X(h_x)$ denotes the distribution of χ_{ii} for given h_x value, $\mathrm{E}[\cdots]$ the expectation value, and the variance $\mathrm{Var}[X(h_x)] = \mathrm{E}[X(h_x)^2] - \mathrm{E}[X(h_x)]^2$.

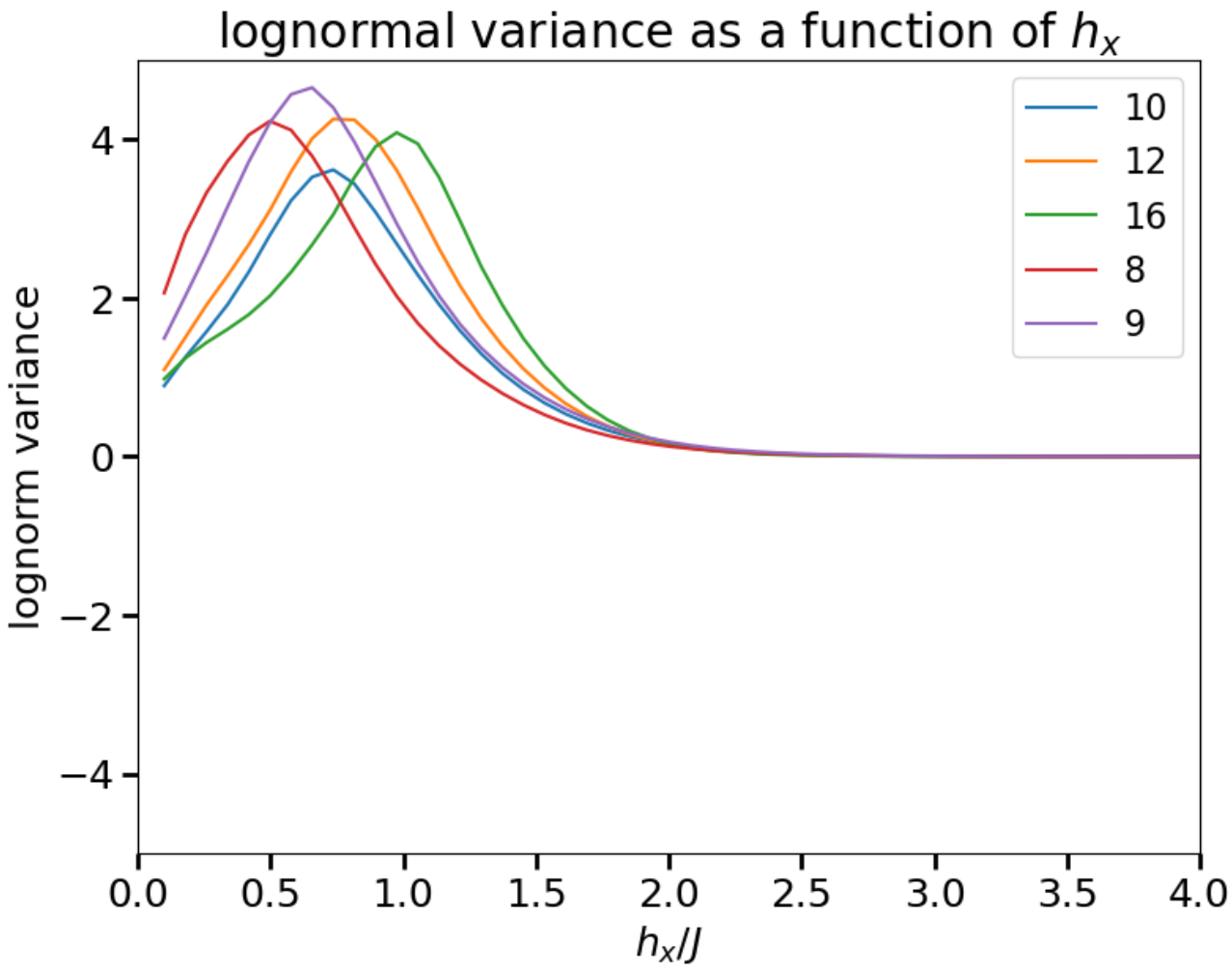

Fig. 5. Lognormal variance of local susceptibility as a function of h_x for systems of $8, 9, 10, 12, 16$ spins. **??**

We also investigate the dependence of critical point—the transverse field value where the spin glass transitions from the Griffiths phase to spin glass phase—upon the different sizes of the system. Although technically, phase transitions only occurs in the thermodynamic limit where the functions of key quantities become singular at the critical point, however, we do observe a more smooth transition behavior in these smaller systems as well. Here, we note the rough transition region from the Griffiths phase—characterized by the long tail—the spin glass phase—characterized by migration of the peak to high local susceptibilities. From the distribution plots, one can roughly see the size dependence of

the transition region.

Table I. The estimated Griffiths-to-spin-glass transition region with respect to size

size	critical region h_x
8	0.896
9	0.896
10	0.976
12	1.135
16	1.135

Although the transition regions above is only qualitatively estimated to human error, it can be argued that the critical region is increasing with respect to the size of the system. In [1], Singh and Young found in 2d cubic lattices the transition point to be around 2.2 using linked cluster expansion method, which is approached from below by our study of critical region of increasing sizes.

III Quantities associated with spin glass

In addition to the distribution of local susceptibility, we also calculate various quantities of interest and make size comparisons. These quantities are ground energy, first-excited energy, entanglement entropy, global susceptibility (as opposed to local susceptibility), and structure factor. We first briefly review the formulas. The ground energy and first-excited energy are readily available after diagonalization. The spin glass susceptibility is defined as

$$\chi_{\text{SG}} = \left[\sum_{\langle i,j \rangle} \chi_{ij}^2 \right]_{\text{disorder}} . \tag{14}$$

where $[\dots]_{\text{disorder}}$ denotes averaging over the disorder in bond configurations. Here χ_{ij} is the local susceptibility calculated from applying longitudinal field over two spins i and j, which comes out of the multivariate Taylor expansion of the ground energy with longitudinal perturbation

$$\begin{aligned} E_0(\{h_z^i\}) &= E_0(\{h_z^i\} = 0) + \sum_i^N \frac{\partial E_0(\{h_z^i\})}{\partial h_z^i} h_z^i - \frac{1}{2} \sum_{i,j}^N \frac{\partial E_0^2(\{h_z^i\})}{\partial h_z^i \partial h_z^j} h_z^i h_z^j \\ &= E_0(\{h_z^i\} = 0) - \frac{1}{2} \sum_{i,j}^N \chi_{ij} h_z^i h_z^j. \end{aligned} \tag{15}$$

Conveniently setting all other longitudinal field values to zero besides the ones on site i and site j and $h_z^i = h_z^j = h_z$, we can rewrite Eq. (15) as

$$E_0(h_z) = E_0(0) - \frac{h_z^2}{2}(\chi_{ii} + \chi_{jj} + 2\chi_{ij})$$
$$\chi_{ij} = \frac{E_0(0) - E_0(h_z)}{h_z^2} - \frac{1}{2}(\chi_{ii} + \chi_{jj}). \tag{16}$$

The structure factor, also know as spin-spin correlation function, measures how much the spins are correlated (i.e. if one spin gets flips, how many others are affected), which requires knowing the wavefunction. It is defined as

$$S_{\text{SG}} = \sum_{i,j} |S_{ij}|^2 \tag{17}$$

where $S_{ij} \equiv \langle \psi_0 | \sigma_i^z \sigma_j^z | \psi_0 \rangle$.

In Fig. (6), we plot the first excited energy and ground state energy.

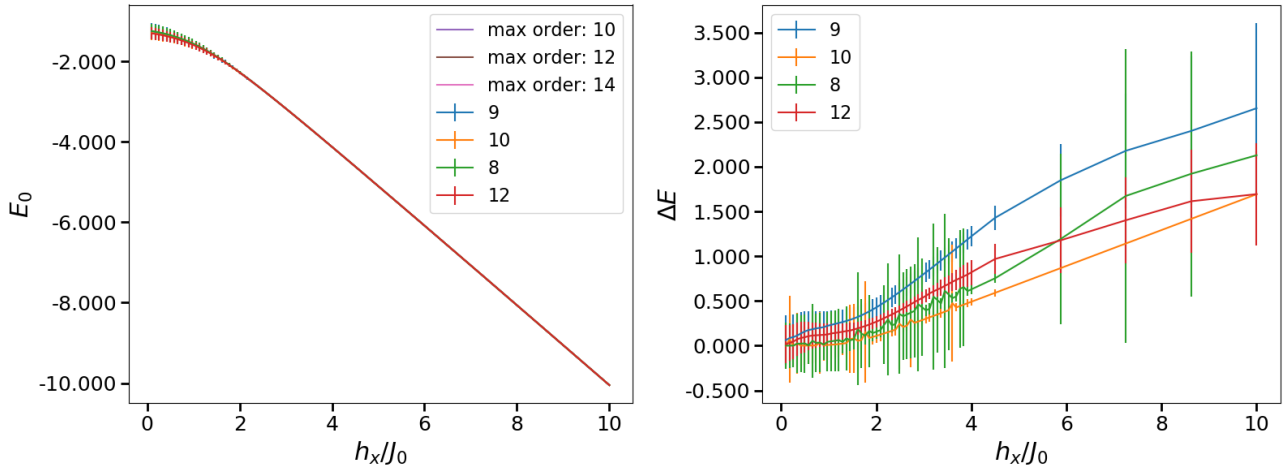

Fig. 6. ground energy (*left*) and first energy gap (*right*) with respect to the transverse field value with errorbars for various system sizes, which is given by the standard deviation of the disorder average.

In Fig. (7), one can see that the transition region of the susceptibility and structure factor gradually approaching 2.2 as the system size scales up. Notably we also see that the disorder standard deviation starts out as being very large and quickly diminishes as the transition happens. At high fields, we expect the spin glass susceptibility as well as the structure factor to be essentially size independent since the Hamiltonian is dominated by transverse field term.

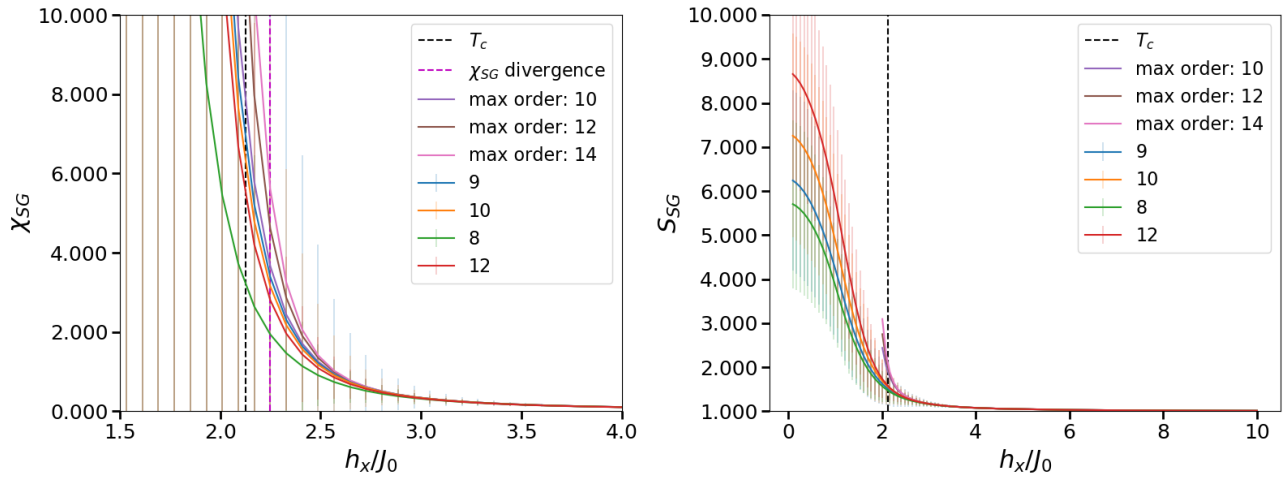

Fig. 7. spin glass susceptibility (*left*) and structure factor (*right*) with respect to the transverse field value with errorbars for various system sizes, which is given by the standard deviation of the disorder average.

In Fig. (8), the disorder-partition averaged entanglement entropy is plotted against the transverse field strength. At low fields, we can see that the total entanglement entropy scales are mostly size-independent—they are $\log(2)$ plus some additional mixture. The 9 spin system is a bit of an odd case since there is no even bipartition. At high fields, again we see that entanglement entropy drops down to zero as the quantum term dominates and the spins become essentially decoupled from each other. Technically there ought to be an area law—meaning that the entropy should scale as square root of N (here area is the abstract concept: imagine the 2d volume of the system being N, then the area is naturally $\sqrt{N}$), but this effect is not obvious for small size systems.

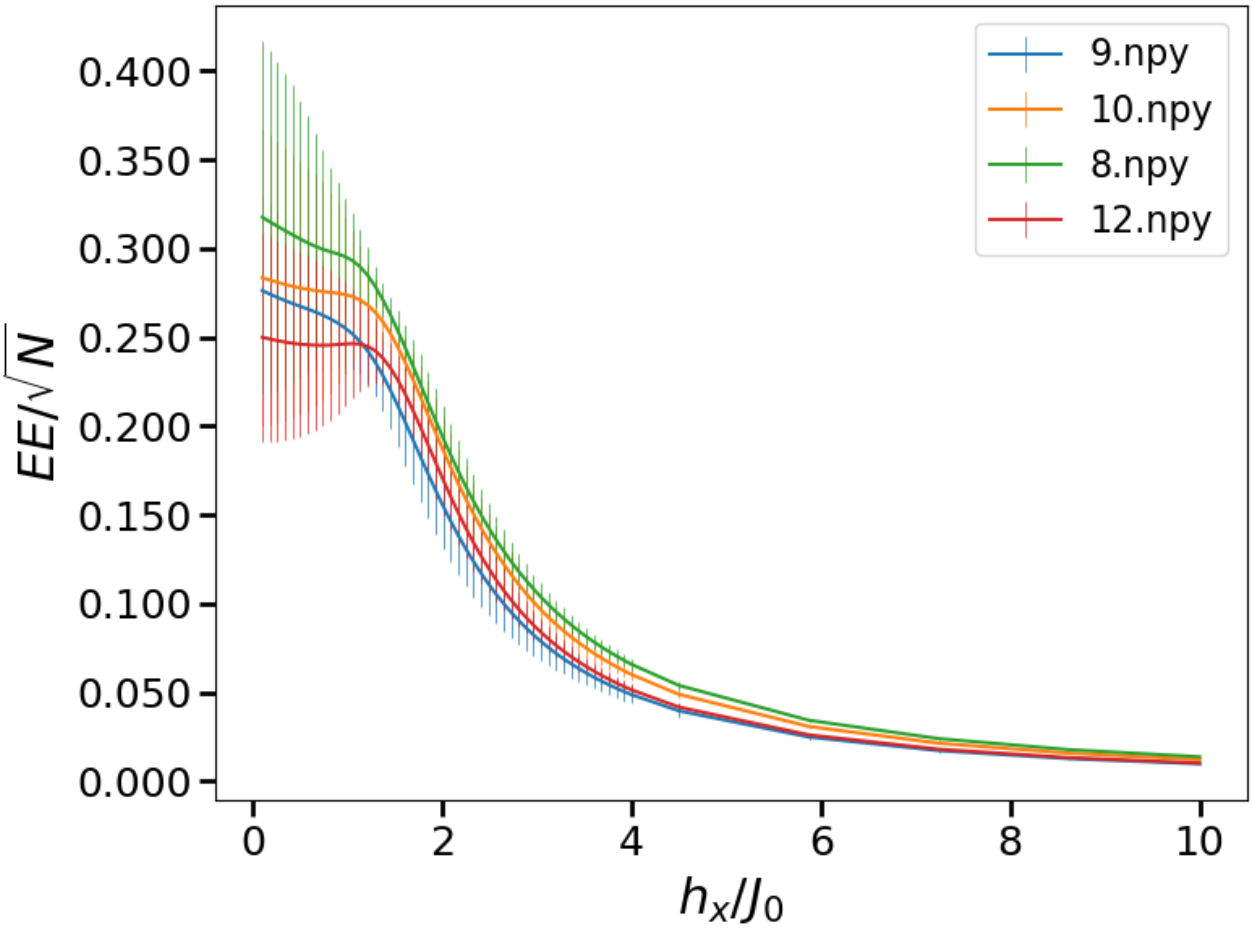

Fig. 8. disorder-partition averaged entanglement entropy with respect to the transverse field value with errorbars for various system sizes, which is given by the standard deviation of the disorder average.

IV Perturbation Theory and Entanglement Entropy

As a side project, we have successfully merged the perturbation theory effective Hamiltonian method with the algorithm to fast-generate the ground states of the system. The goal is to use the Effective Hamiltonian method to perturbatively approximate the spatial bipartition-averaged entanglement entropy at the low field limit for system sizes much larger than what is typically possible for the Lanczos algorithm, thereby enabling us to statistically study the entanglement entropy distribution for a large number of randomly generated spin glasses. However, the entanglement entropy as given by this perturbation theory calculation remains somewhat unstable as sometimes we run into issues with machine precision, In particular, when the two lowest-lying energies are so close to each other that the

machine confuses the two states for different h_x values. This causes the entanglement entropy to fluctuate fiercely between two different curves. Aside from this, the major drawbacks of using effective Hamiltonian method to study entanglement entropy include 1) the transverse field region in which the entanglement entropy is well-approximated is very limited, 2) although the algorithm for generating ground states and calculating the effective Hamiltonian allows for large system sizes, since the size of the ground manifold scales linearly with the size of the system and fluctuates wildly depending on the bond configurations, it may happen that the ground manifold is not connected at 4th order perturbation theory (the order at which our implementation of algorithm currently sits) in which the perturbation theory is no longer reliable. Thus, in this method, the set of spin glasses that we are able to study is still limited to those ones with ground manifold small enough for fourth order perturbation theory and with an energy gap between the ground energy and the first excited energy large enough that does not challenge machine precision.

remains as a future endeavor to write an algorithm that finds the plateau region of the entanglement entropy and perform disorder averaging. Then we can finally study the size dependence of the entanglement entropy for sizes larger than what is possible for the Lanczos algorithm at the low-field limit. Besides the low-field limitations, we should note that there is a size limitation also since the ground manifold must not be large enough such that it becomes disconnected as fourth order perturbation.

V Perturbation Theory Susceptibility

We also attempted to use perturbation theory to study susceptibility in the low-field limit, but this attempt turned out to be unsuccessful due to computational cost: the additional added Pauli-z operator is also needed to be expanded in the perturbation expansion and needs to be re-built for each site.

Acknowledgments

This work is conducted under the help and guidance of Dr. Rajiv Singh at UC Davis, using the code base originally developed by Dr. Chris Herdman. The algorithm for fast-generating the ground states is developed by Ellie Copps, and finalized by Jack Landrigan of Middlebury College.

References

[1] R. R. P. Singh and A. P. Young, "Critical and griffiths-McCoy singularities in quantum ising spin glasses on mml:math xmlns:mml="http://www.w3.org/1998/math/MathML"mml:mid/mml:mi/mml:math -dimensional hypercubic lattices: A series expansion study," *Physical Review E*, vol. 96, aug 2017.